8-5-2010

Residue Mutations in [Fe-Fe]-Hydrogenase Impedes O 2 Binding: A QM/MM Investigation

Daniela Dogaru
Cleveland State University

Stefan Motiu
Cleveland State University

Valentin Gogonea
Cleveland State University, V.GOGONEA@csuohio.edu

Publisher's Statement

This is the accepted version of the following article: Dogaru, D.; Motiu, S.; Gogonea, V. Residue mutations in [Fe Fe]-hydrogenase impedes O2 binding: A QM/MM investigation. International Journal of Quantum Chemistry 2010, 110, 1784-1792. ., which has been published in final form at http://onlinelibrary.wiley.com/doi/10.1002/qua.22331/abstract

Residue Mutations in [Fe—Fe]-Hydrogenase Impedes O_2 Binding: A QM/MM Investigation

DANIELA DOGARU, STEFAN MOTIU, VALENTIN GOGONEA

Introduction

[Fe—Fe]-hydrogenases are enzymes that catalyze the reversible reduction of protons to molecular hydrogen ($2H^+ + 2e^- \rightleftarrows H_2$) in anaerobic media [1, 2], and are considered one of the oldest enzymes in nature [3]. The eventual elucidation of the catalytic mechanism of hydrogen synthesis may avail researches produce clean hydrogen fuel, using certain prokaryotes and eukaryotes [4–13].

The active site of hydrogenase, the H-cluster (Scheme 1) is composed of two iron atoms (Fe_p—Fe_d, i.e., proximal and distal iron). The di-iron atoms are coordinated by endogenous ligands, i.e., two cyanides, two terminal carbonyls, and a bridging carbonyl (CO_b). Also, 1,3-di(thiomethyl)-amine (DTMA) and propanedithiolate (PDT) are bidentate ligands of the di-iron subsite [14–16]. A cubane cluster, [4Fe—4S] (which also belongs to the H-cluster), is bonded to S_γ of Cys^{382}, while the former (S_γ) is bound to Fe_p of the H-cluster.

Previous density functional theory (DFT) as well as hybrid quantum mechanics/molecular mechanics (QM/MM) calculations [1, 17–23] have been successful in clarifying some aspects of the catalytic properties of the H-cluster. As in previous computational studies [1, 18], CH_3—S is substituted for cysteine, and a H^+ replaces the proximal cubane. Furthermore, computational and experimental research [1, 14, 24–52] on [Fe—Fe]-hydrogenase H-cluster and synthetic H-cluster-like compounds sheds light on the potential redox states of the [Fe—Fe]-hydrogenase H-cluster subunit, Fe_p—Fe_d; Fe_p^I—Fe_d^I is the reduced hydrogenase H-cluster

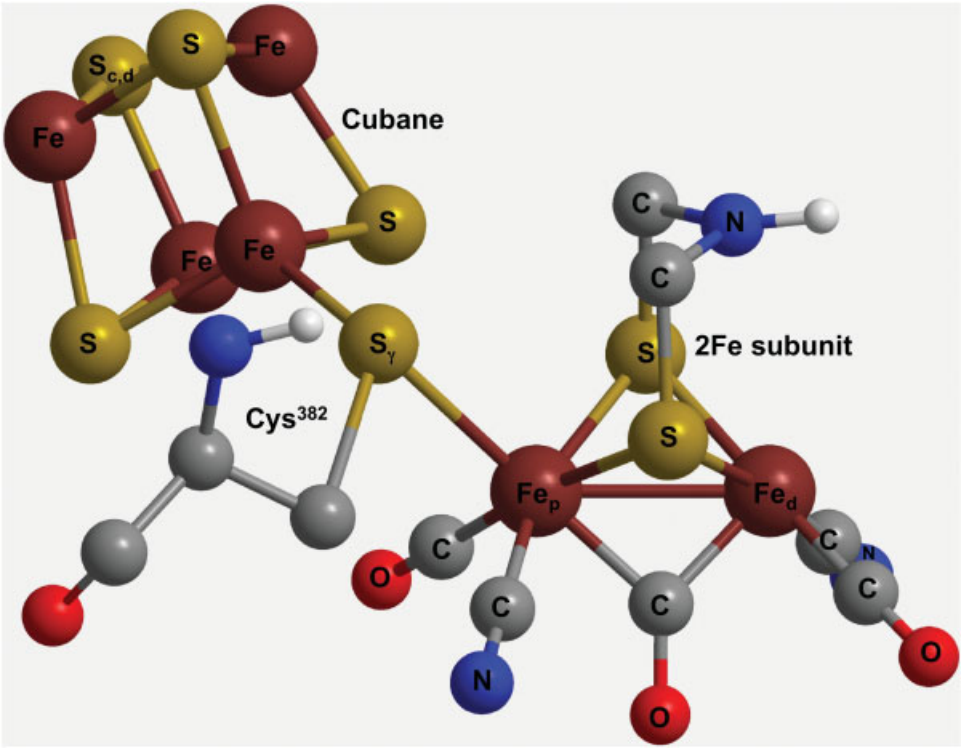

SCHEME 1. The H-cluster with its proximal cubane and 2Fe subcluster. [Color figure can be viewed in the online issue, which is available at www.interscience.wiley.com.]

subunit, Fe_p^{II}—Fe_d^{I} is the partially oxidized enzyme subunit, and Fe_p^{II}—Fe_d^{II} is the fully oxidized, inactive enzyme H-cluster subunit.

The oxidized H-cluster, Fe_p^{II}—Fe_d^{II}, has OOH^-, H_2O molecule, or OH^- bound to the Fe_d^{II} site [18, 24]. In our previous investigation [31], we have inferred that a vacant Fe_p^{II}—Fe_d^{II} could also be a viable intermediate in H_2 synthesis. Regardless of the redox states in [Fe—Fe]-hydrogenase H-cluster, the proximal cubane always retains a 2+ oxidation state, $[Fe_4S_4]^{2+}$. The partially oxidized H-cluster (containing Fe_p^{II}—Fe_d^{I}), H_{ox}, is the active species of the hydrogenase enzyme having the tendency for protonation (Liu and Hu [18]).

The crystal structures of hydrogenase obtained from *Clostridium pasteurianum* (CP) [15] and *Desulfovibrio desulfuricans* (Dd) [16] led to a more detailed understanding of the biochemical role of these enzymes. The crystal structure of CPI hydrogenase shows an oxygen species (i.e., either OH^- or H_2O) bound to Fe_d. However, according to the X-ray crystal structure of CPI, and based on computational results of Tye et al. [24], the enzyme has OOH^- bound to Fe_d in its inactive form. Hence, we endeavor to ascertain if oxygen binding to distal iron (Fe_d—O_2) can be hindered by residue mutations within the surrounding apoprotein of the catalytic site.

The current investigation comprised two subdivisions: (1) The thermodynamic analysis of the reactions of O_2 binding to wild-type and mutated [Fe—Fe]-hydrogenase for the three different oxidation states of the di-iron subcluster: Fe_p^{I}—Fe_d^{I}, Fe_p^{II}—Fe_d^{I}, and Fe_p^{II}—Fe_d^{II}. (2) Geometrical analyses of interatomic distances in Fe_d—O_2, the extrinsic ligand, O—O, and of CO_b carbon distances to the di-iron atoms. In the Supporting Information, the NBO charges and an electronic analysis discussing the frontier molecular orbitals are presented.

Methods

The QM/MM (DFT/UFF [53]) ONIOM [54] method (DFT for the QM region, and the universal force field, UFF, for the MM region, implemented in Gaussian03 [55]) has been used to calculate the reaction thermodynamics, i.e., ΔG, for the reactions of oxygen binding to [Fe—Fe]-hydrogenase. The electronic structure of H-cluster (except the proximal cubane) was described by QM using the DFT Hamiltonian (B3LYP functional [56, 57]), with 6-31+G(d,p) basis set. In accordance with experimental and in silico data, low spin states (singlet, and doublet) and low oxidation states (I, and II) have been selected for the Fe atoms [1, 23].

The Gromacs program [58, 59] was used to add hydrogen atoms, water, and counter ions to the crystal structure of DdH [Brookhaven Protein Data Bank (id.1HFE)]. A 1 nm layer of water has been added to the DdH structure. Sodium cations have been randomly inserted into the solvent to neutralize the negative charges encountered in DdH, e.g., the −2 a.u. found on the cubane/cysteine moieties, or in the H-cluster (when needed) [60]. For both basic and acidic amino acids, charges were assigned by the Gromacs program pdb2gmx to be at pH 7. The low layer consists of all metalloenzyme residues as well as its constituent cubanes, i.e., proximal, medial, and distal. The high layer comprised 2Fe subunit, (which is a moiety of the H-cluster), and C_β and S_γ (of the bridging Cys^{382}). Two linking hydrogen atoms were added between C_α and C_β of Cys^{382}, and between S_γ and a Fe atom of the proximal cubane. The charge equilibration method of the UFF was used to describe the electrostatic interactions within the low layer of the system [61]. The DdH partial charges were obtained using the charge equilibration method (QEq), whereas the solvent charges were acquired from literature [61] ($q_O = -0.706$ a.u. and $q_H = 0.353$ a.u.).

ONIOM geometry optimizations have been performed on DdH, with the low layer (MM region) being frozen[2], with the exception of the proximal cubane; for the high layer (QM), only the iron atoms, Fe_p—Fe_d, and the N (of the DTMA bridge) have been kept frozen[3].

Residue mutations were carried out within the adjacent apoenzyme environment to the H-cluster in order to hinder O_2 from binding to the open coordination site (Fe_d) of DdH H-cluster. Residue mutations are composed of deletions and substitutions, which are performed 8 Å radially outward from Fe_d. To screen the 30 polar residues located in the 8 Å apoenzyme layer, individual residue deletions were carried out followed by calculations to ascertain what residue substitutions should be

[2]Where "frozen" means that x, y, z atom coordinates are kept fixed; "freezing atoms" is practiced to reduce the computational time.

[3]For the fully and partially oxidized vacant di-iron subunits, additional optimizations have been carried out by freezing these atoms: Fe_p—CO_t (where CO_t stands for terminal carbonyl; CO_t is bound to Fe_p). The extra optimizations have been done because the above-mentioned di-iron subunits are more likely to undergo CO_b migration.

made to impede O_2 binding to Fe_d. The deletion of a residue was performed by removing the point charges of its atoms from the Gaussian input file. Residue deletions and substitutions were performed for all three di-iron subcluster oxidation states of [Fe—Fe]-hydrogenase H-cluster: Fe_p^{II}—Fe_d^{II}, Fe_p^{II}—Fe_d^{I}, and Fe_p^{I}—Fe_d^{I}.

Results and Discussion

THERMODYNAMICS OF O_2 BINDING TO [Fe—Fe]-HYDROGENASE H-CLUSTER IN GAS PHASE AND PROTEIN ENVIRONMENT

Calculations in Gas Phase and in Wild-Type Enzyme Environment

The results of the QM/MM calculations for the reactions of O_2 binding to [Fe—Fe]-hydrogenase are shown in Table I. Two values of the Gibbs energy are given for wild-type DdH. In the first row are Gibbs energies ($\Delta G^c_{QM/MM}$) obtained by taking into account neighboring charges of the 2Fe subunit: i.e., point charges from the proximal cubane [4], the MM region of Cys^{382}, C of the peptide bond in Gly^{381}, and N of Val^{383}. The values ($\Delta G_{QM/MM}$) in the second row of Table I were obtained without including the neighboring charges of the 2Fe subunit in the calculation. Sometimes the deletion of MM charges in the vicinity of the QM system is necessary to avoid distortions (artificial polarization) in the wave function induced by these charges. The difference in the wave function polarization (i.e., with or without neighboring charges) is quantified by difference in the natural bond orbital charges [NBO, Figs. 1(a) and (b)]. The strongest effect of the neighboring MM charges is on the NBO charges of S_γ of Cys^{382} and the linking atom (H_L) attached to it. A detailed analysis of these charges is given in the Supporting Information.

Figure 2 shows O_2 inhibition pathways for all three oxidation states of the H-clusters: Fe_p^{II}—Fe_d^{II} (1), Fe_p^{II}—Fe_d^{I} (3), and Fe_p^{I}—Fe_d^{I} (5), where (1), (3), and (5), are the cluster identifiers. In gas phase, the 1st reaction, $1 \rightarrow 2$, (O_2 binds to the fully oxidized H-cluster (1)) is endergonic ($\Delta G_{gas} = +9.8$ kcal/mol; gas = gas phase [5]). Hybrid QM/MM calculations, on the other hand, show that O_2 binding in protein environment occurs exergonically ($\Delta G^c_{QM/MM} = -16.6$ kcal/mol; $\Delta G_{QM/MM} = -10.6$ kcal/mol), confirming the affinity of hydrogenases for O_2 [62].

In gas phase, the 2nd reaction, $3 \rightarrow 4$, starts with the partially oxidized H-cluster (3), Fe_p^{II}—Fe_d^{I}, and the bonding of O_2 to Fe_d^{I} occurs rather exergonic ($\Delta G_{gas} = -36.1$ kcal/mol). ONIOM results show that in protein environment O_2 binds spontaneously to the H-cluster when neighboring charges are included (Fe_p^{II}—Fe_d^{I}, $\Delta G^c_{QM/MM} = -7.9$ kcal/mol), but the binding reaction is nonspontaneous

TABLE I

Gibbs energies (kcal/mol) for O_2 binding to wild-type DdH and to DdH modified by residue removal.

Reaction	FeII—FeII + O_2	FeII—FeI + O_2	FeI—FeI + O_2
Wild-type DdH[a]	−16.6	−7.9	−20.7
Wild-type DdH	−10.6	+2.6	−20.5
ΔSer^{62b}	−9.0	+2.5	−20.4
ΔArg^{111}	−11.2	+2.2	−22.9
ΔTyr^{112}	−10.8	−3.2	−21.1
ΔAsp^{144}	−8.4	+4.6	−20.5
ΔThr^{145}	−11.1	+3.9	−21.5
ΔGlu^{146}	−8.7	+2.7	−21.6
ΔThr^{148}	−10.9	+2.1	−21.2
ΔAsp^{150}	−9.4	+1.9	−22.8
ΔThr^{152}	−9.2	+4.1	−18.6
ΔGlu^{155}	−11.1	+2.2	−21.0
ΔThr^{176}	−10.1	+3.0	−19.6
ΔSer^{177}	−10.8	+4.4	−21.3
ΔGln^{183}	−10.8	+2.9	−19.7
ΔSer^{198}	−10.5	+2.7	−20.3
ΔLys^{201}	−10.6	+2.5	−20.9
ΔSer^{202}	−7.9	+3.9	−17.3
ΔAsn^{207}	−10.3	+2.6	−21.1
ΔSer^{230}	−10.3	+2.9	−19.8
ΔLys^{237}	−10.0	−2.7	−24.5
ΔLys^{238}	−11.7	+2.2	−21.0
ΔGlu^{240}	−10.7	+3.6	−20.9
ΔThr^{257}	−10.7	−2.9	−20.5
ΔThr^{259}	−11.2	−3.0	−20.7
ΔThr^{260}	−10.5	+2.7	−20.3
ΔSer^{289}	−10.3	−2.9	−20.7
ΔThr^{294}	−10.1	+3.2	−20.1
ΔThr^{299}	−10.5	−2.8	−20.5
ΔGlu^{374}	−10.1	+4.7	−21.5
ΔTyr^{375}	−10.4	+2.7	−20.7
ΔGln^{388}	−10.8	+2.5	−20.4

[a] Gibbs energies for the wild-type enzyme; the MM layer includes the neighboring point charges of 2Fe subunit, viz., over proximal cubane (except $S_{c,d}$), MM section of Cys^{382}, C (of the peptide bond) from Gly^{381}, and over N of Val^{383}.
[b] Residue removed from small chain of DdH.

[4]Except for the cubane sulfur ($S_{c,d}$) situated diagonally from the cubane Fe (bound to cysteinyl sulfur of Cys^{382}).

[5]The gas phase results are reproduced from Ref. [17].

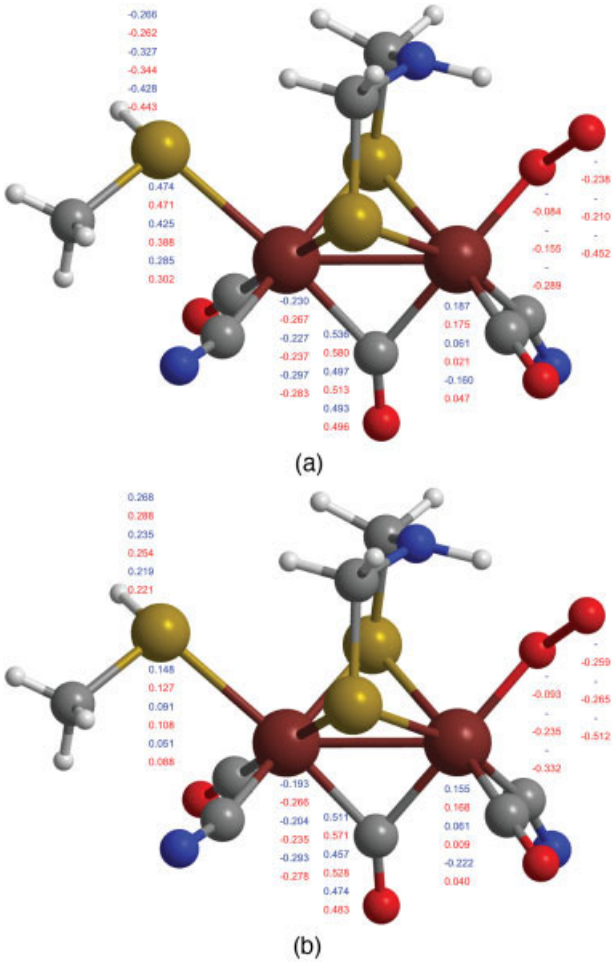

FIGURE 1. NBO charges of 2Fe subunit with and without (MM layer) neighboring charges. [Color figure can be viewed in the online issue, which is available at www.interscience.wiley.com.]

($\Delta G_{QM/MM}$ = +2.6 kcal/mol) when the neighboring charges are not included.

The 3rd reaction in gas phase, 5 → 6, starts with the reduced H-cluster (5), Fe_p^I—Fe_d^I; the reaction occurs spontaneously (ΔG_{gas} = −36.0 kcal/mol) and has almost identical Gibbs energy as reaction 3 → 4, probably because both loci of oxygen binding (Fe_d^I—O_2) are on similar oxidized species, Fe_d^I. However, the QM/MM calculations for 5 → 6 show a difference between the enzyme ($\Delta G^c_{QM/MM}$ = −20.7 kcal/mol; $\Delta G_{QM/MM}$ = −20.5 kcal/mol) and gas phase results (ΔG_{gas} = −36.0 kcal/mol) Gibbs energies.

In Figure 2, the gas phase protonation reaction 5 → 7 is very exergonic (ΔG_{gas} = −220.6 kcal/mol), essentially because the charge on H-cluster 5 is −2 a.u. ONIOM calculations also show a very high H^+ affinity ($\Delta G^c_{QM/MM}$ = −219.2 kcal/mol) for the hydrogenase H-cluster, which is close to the gas phase result (ΔG_{gas} = −220.6 kcal/mol). The thermodynamic results in Figure 2 demonstrate that most reactions considered for the hydrogenase H-cluster proceed exergonically with the exception of 1 → 2 in gas phase. Thus, the calculations on the wilde-type [Fe—Fe]-hydrogenase are in agreement with experimental observations and confirm the inhibition of [Fe—Fe]-hydrogenase by molecular oxygen.

Calculations in Mutated Enzyme Environment

The thermodynamic calculations of O_2 binding to the H-cluster in gas phase and protein environ-

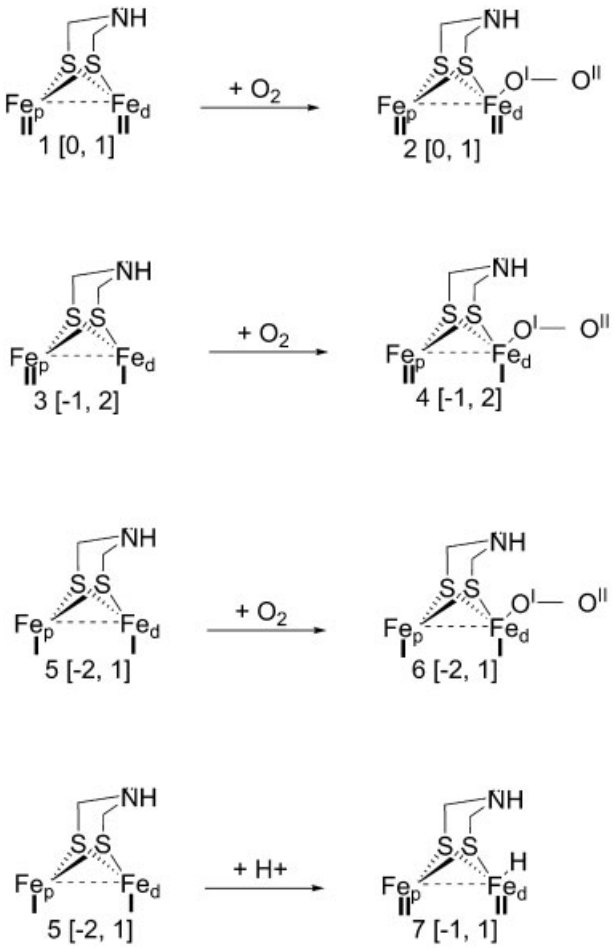

FIGURE 2. Oxidation reactions of O_2 with the fully oxidized (1), partially oxidized (3), and reduced (5) di-iron subunits. Also the protonation with the reduced (5) di-iron subunit is depicted. The charge and multiplicity are provided in square brackets.

ment suggest that the enzyme electric field modulates the reactivity of the H-cluster toward O_2, and thus is responsible for the inhibition of [Fe—Fe]-hydrogenase by molecular oxygen. Thus, thoughtful modification of the enzyme electric field by residue mutation may advert or weaken the O_2 binding to the H-cluster. This idea is the basis of the study presented here.

Residue screening in a protein layer (8 Å) surrounding the H-cluster has been carried out to gauge the effect of point mutations on the strength of O_2 binding to H-cluster. First, we performed residue deletions to gauge the effect of the electric field of the residues targeted for substitution on the reaction of O_2 binding, and then we performed residue substitutions for residues that showed significant effect upon deletion.

For O_2 binding to Fe_d^{II} (of the oxidized biferrous hydrogenase H-cluster subsite, Fe_p^{II}—Fe_d^{II}, (1)), the results obtained are a function of stereoelectronic effects from the juxtaposed residues on the catalytic site. Both neutral polar and charged residue deletions provided good results, e.g., ΔSer [62]s[6], ΔAsp^{144}, ΔGlu^{146}, ΔAsp^{150}, ΔThr^{152}, and ΔSer^{202} gave $\Delta G_{QM/MM} = -9.0$ kcal/mol, $\Delta G_{QM/MM} = -8.4$ kcal/mol, $\Delta G_{QM/MM} = -8.7$ kcal/mol, $\Delta G_{QM/MM} = -9.4$ kcal/mol, $\Delta G_{QM/MM} = -9.2$ kcal/mol, and $\Delta G_{QM/MM} = -7.9$ kcal/mol, respectively.

O_2 is hindered from binding to Fe_d^{I} of the partially oxidized di-iron subsite (Fe_p^{II}—Fe_d^{I}). Endergonic binding reactions have been identified all tried residue deletions (Table I), except for the following: ΔTyr^{112}, ΔLys^{237}, ΔThr^{257}, ΔThr^{259}, ΔSer^{289}, and ΔThr^{299}, which gave $\Delta G_{QM/MM} = -3.2$ kcal/mol, $\Delta G_{QM/MM} = -2.7$ kcal/mol, $\Delta G_{QM/MM} = -2.9$ kcal/mol, $\Delta G_{QM/MM} = -3.0$ kcal/mol, $\Delta G_{QM/MM} = -2.9$ kcal/mol, and $\Delta G_{QM/MM} = -2.8$ kcal/mol, respectively.

An improved trend toward impeding O_2 binding to Fe_d^{I}, of the fully reduced di-iron subsite (Fe_p^{I}—Fe_d^{I}), has been observed for residue deletions (Table I): ΔThr^{152} and ΔSer^{202}, which gave $\Delta G_{QM/MM} = -18.6$ kcal/mol, and $\Delta G_{QM/MM} = -17.3$ kcal/mol, respectively. Table I shows that the deletion of charged amino acid residues like Asp^{144} and Glu^{374} has a similar effect ($\Delta G_{QM/MM} = +4.6$ and +4.7 kcal/mol, respectively) on O_2 binding to Fe_p^{II}—Fe_d^{I}, as the deletion of polar but neutral amino acid residues like Thr^{152} and Ser^{202} ($\Delta G_{QM/MM} = +4.1$ and +3.9 kcal/mol, respectively), which seems rather intriguing. A closer look at the distribution of the amino acid residues targeted for deletion in the 8 Å layer around the di-iron catalytic unit reveals that the charged residues Asp^{144} and Glu^{374} are about 10 Å away from distal Fe, while Thr^{152} and Ser^{202} are about 3 Å closer. This difference in location with respect to the H-cluster explains why the deletion of two charged residues, further away, has a similar effect on O_2 binding as the deletion of two polar residues, which are much closer to H-cluster. The residues interlaced between Asp^{144}/Glu^{374} and the catalytic site screen the bare charge of these charged residues, thus diminishing its effect on the electronic structure of the di-iron unit. Because charged residues have a stronger effect on their local environment than polar residues, it is expected that polar/nonpolar residues are better targets for mutations because their replacement should be less detrimental to the overall folding of the enzyme. Thus, we selected neutral polar residues for mutations.

With the positive results obtained from residue deletions, we were now able to carry out residue substitutions (Table II). Two residue deletions (ΔThr^{152} and ΔSer^{202}), which showed significant effect on the Gibbs energy of O_2 binding for all oxidation states of the di-iron H-cluster subunit, were followed by mutations to alanine, i.e., Thr^{152}Ala and Ser^{202}Ala. The dual residue deletions, ΔThr^{152} and ΔSer^{202}, impede further O_2 binding to the H-cluster subunit Fe_p^{II}—Fe_d^{I} ($\Delta G_{QM/MM} = +5.4$ kcal/mol). However, for the oxidation states Fe_p^{II}—Fe_d^{II} and Fe_p^{I}—Fe_d^{I}, only a slight enhancement in O_2 inhibition has been observed (+2.2 and +4.4 kcal/mol, respectively). The simultaneous mutations to alanine (Thr^{152}Ala and Ser^{202}Ala) give better O_2 inhibition results ($\Delta G_{QM/MM} = -9.2$ kcal/mol for Fe_p^{II}—Fe_d^{II}, $\Delta G_{QM/MM} = +4.2$ kcal/mol for Fe_p^{II}—Fe_d^{I}, and $\Delta G_{QM/MM} = -18.1$ kcal/mol for Fe_p^{I}—Fe_d^{I}).

TABLE II

Gibbs energies (kcal/mol) for O_2 binding to wild-type DdH and to DdH modified by residue deletion.

Reaction	FeII—FeII + O_2	FeII—FeI + O_2	FeI—FeI + O_2
Wild-type DdH	−10.6	+2.6	−20.5
ΔThr^{152}, ΔSer^{202}	−8.4	+5.4	−16.1
ΔThr^{152}, ΔSer^{202} (at 100°C)	−5.6	+7.9	−12.9
Thr^{152}Ala, Ser^{202}Ala	−9.2	+4.2	−18.1

[6]s = DdH small chain.

TABLE III

Geometrical results for wild-type DdH H-cluster. Interatomic distances (Å) between Fe_p and CO_b, Fe_d and CO_b, Fe_d and O_I, and O_I—O_{II}, and the angle Fe_d—O_I—O_{II} before and after O_2 binding.

	$Fe^{II}Fe^{II}$	$Fe^{II}Fe^{I}$	$Fe^{I}Fe^{I}$
Before O_2 binding			
Fe_p—CO_b	1.925	1.939	1.942
Fe_d—CO_b	1.942	1.908	1.826
After O_2 binding			
Fe_p—CO_b	1.807	1.924	1.935
Fe_d—CO_b	2.287	1.924	1.945
O_I—Fe_d	1.729	1.840	1.808
O_I—O_{II}	1.276	1.281	1.373
Fe_d—O_I—O_{II}	137.0	160.6	126.0

Additionally, it is known that certain organisms containing [Fe—Fe]-hydrogenases thrive around subocean thermal vents [3]. Hence, at a temperature of 100°C intercalated with hydrogenase mutations (Table II), QM/MM results indicate that the extrinsic O_2 binding to metalloenzyme is further reduced ($\Delta G_{QM/MM} = -5.6$ kcal/mol for Fe_p^{II}—Fe_d^{II}, $\Delta G_{QM/MM} = +7.9$ kcal/mol for Fe_p^{II}—Fe_d,^{I} and $\Delta G_{QM/MM} = -12.9$ kcal/mol for Fe_p^{I}—Fe_d^{I}).

DdH GEOMETRICAL READJUSTMENT UPON OXIDATION

In this section, the Gibbs energies for the reaction of O_2 binding to wild-type DdH are correlated with geometrical parameters such as interatomic distances and bond angles (Table III). The iron-carbon distances in the Fe_p—CO_b subunit are investigated for all three oxidation states of the di-iron subunits.

The iron-carbon distance in Fe_p—CO_b (Fe_p^{II}—Fe_d^{II}) becomes smaller, 1.925 Å (1) → 1.807 Å (2), upon O_2 binding concomitant with Fe_d—CO_b bond elongation, 1.942 Å (1) → 2.287 Å (2), which generally indicates an increased bonding strength for an exogenous ligand [31] (i.e., O_2). For Fe_p^{II}—Fe_d^{I}, the bond distance Fe_p—CO_b becomes smaller, 1.939 Å (3) → 1.924 Å (4), upon O_2 binding while a bond elongation is observed for Fe_d—CO_b, 1.908 Å (3) → 1.924 Å (4). For the reduced di-iron subcluster (Fe_p^{I}—Fe_d^{I}) the bond distance Fe_p—CO_b becomes smaller, 1.942 Å (5) → 1.935 Å (6), upon O_2 binding, while Fe_d—CO_b increases, 1.826 Å (5) → 1.945Å (6). The above geometrical analysis concludes that for all oxidation states of Fe_p—Fe_d the bond between the carbon of the bridging carbonyl (CO_b) and Fe_d becomes longer and the bond between CO_b and Fe_p becomes shorter, upon O_2 binding to the catalytic site.

Next, an analysis is presented for the interatomic distances between distal iron and oxygen, and between oxygen atoms, relative to Gibbs energy of O_2 binding to all three di-iron oxidation states.

For the Fe_p^{II}—Fe_d^{II} subcluster, the iron-oxygen distance, Fe_d—O_I, is rather small (1.729 Å; Table III), which suggests a strong bonding ($\Delta G_{QM/MM} = -10.6$ kcal/mol; 1 → 2) between the distal iron and the oxygen atom bound to it. The interoxygen (O_I—O_{II}) bond distance is 1.276 Å, which corresponds to a bond order between a single and double bond.

In the case of the active di-iron subcluster, Fe_p^{II}—Fe_d^{I}, the Fe_d—O_I bond distance is ca. 6% longer (1.840 Å) than Fe_d—O_I interatomic distance in Fe_p^{II}—Fe_d^{II}—O_I, giving rise to a weaker bond ($\Delta G_{QM/MM} = +2.6$ kcal/mol; 3 → 4) between the distal iron and oxygen. The O_I—O_{II} bond distance is 1.281 Å, which is relatively close to the O_I—O_{II} bond for Fe_p^{II}—Fe_d^{II} subcluster.

In Fe_p^{I}—Fe_d^{I}, the O_I—O_{II} bond distance is relatively larger, 1.373 Å, which suggests that π-backdonation occurs between a filled *d*-orbital of Fe_d and the empty π^*orbital of O_2. Out of the three di-iron oxidation states, only the reduced di-iron subcluster (Fe_p^{I}—Fe_d^{I}) has attributes of π-backdonation [7], i.e., the O_I—O_{II} bond order is intermediate between a double and a single bond order, and the O_I—O_{II} bond is elongated (1.373 Å).

Finally, the Fe_d—O_I—O_{II} angle varies as the oxidation states decrease: Fe_p^{II}—Fe_d^{II}—O_I—O_{II} (137.0°), Fe_p^{II}—Fe_d^{I}—O_I—O_{II} (160.6°), and Fe_p^{I}—Fe_d^{I}—O_I—O_{II} (126.0°) in conjunction with effects of the nearby electric field of the apoprotein.

[7]The π-backdonation agrees with the Gibbs energy results form Table I. For example, the Fe_p^{II}—Fe_d^{II} subcluster has an exergonic Gibbs energy ($\Delta G_{QM/MM} = -16.6$ kcal/mol), which can be improved however by DdH mutations such as residue deletions and substitutions, since there is only slight π-backdonation present. The bond Fe_d—O_I is still relatively weak ($\Delta G = -7.9$ kcal/mol) for Fe_p^{II}—Fe_d^{I} subsite. However, for the reduced Fe_p^{I}—Fe_d^{I} subsite, the π-backdonation makes the oxygen bond very strong, thus making its elimination rather difficult (even by means of DdH mutations, Table II).

Conclusion

The QM calculations on the gas phase H-cluster in different oxidation states of Fe_p—Fe_d subunit show that O_2 binding to the fully oxidized H-cluster (Fe_p^{II}—Fe_d^{II}) is exergonic, and endergonic for the partially oxidized (Fe_p^{II}—Fe_d^{I}) and reduced (Fe_p^{I}—Fe_d^{I}) H-clusters.

On the other hand, the QM/MM calculations on the wild-type [Fe—Fe]-hydrogenase confirm that the resting state of the enzyme (Fe_p^{II}—Fe_d^{II}) is inhibited by O_2. In addition, the O_2 binding to the partially oxidized (Fe_p^{II}—Fe_d^{I}) hydrogenase is slightly endergonic, but is exergonic for the reduced oxidation state (Fe_p^{I}—Fe_d^{I}). The contrast between the calculation results in gas phase and protein environment suggest a dramatic effect of the enzyme electric field on the O_2 binding reaction. Thus, we explored the modulation of this electric field by performing point mutations in an 8 Å protein layer surrounding the H-cluster. First, residue deletions have been performed, one by one. Then, from clues obtained from these residue deletions, residue substitutions have been carried out. For Fe_p^{II}—Fe_d^{II}, both the neutral polar residue and the charged residue deletions (ΔSer^{62}s, ΔAsp^{144}, ΔGlu^{146}, ΔAsp^{150}, ΔThr^{152}, and ΔSer^{202}) led to a decreased binding of O_2. For Fe_p^{II}—Fe_d^{I} residue deletions ΔGlu^{374}, ΔAsp^{144}, ΔSer^{177}, and ΔThr^{152} and for Fe_p^{I}—Fe_d^{I} residue deletions ΔThr^{152} and ΔSer^{202} hinder O_2 binding to Fe_d^{I}.

As expected, residue substitutions Thr^{152}Ala and Ser^{202}Ala affect O_2 binding to the same extent as the corresponding deletions (ΔThr^{152} and ΔSer^{202}).

Finally, the fact that one substitutes nonpolar amino acid residues (Thr^{152}Ala and Ser^{202}Ala) for some polar ones juxtaposed to the catalytic site (the H-cluster) seems to be sufficient cause to hinder the binding of O_2 to hydrogenase H-cluster. This shows that well thought modulation of the enzyme electric field accomplished by point mutations can be used to advert hydrogenase inactivation by molecular oxygen. Hence, DdH mutations open up new research opportunities along these lines.

ACKNOWLEDGMENTS

Computational resources have been provided by the National Center for Supercomputer Applications (University of Illinois) and the Ohio Supercomputer Center.

References

1. Liu, Z.-P.; Hu, P. J Am Chem Soc 2002, 124, 5175.
2. Das, D.; Dutta, T.; Nath, K.; Kotay, S. M.; Das, A. K.; Veziroglu, T. N. Curr Sci 2006, 90, 1627.
3. Cammack, R.; Frey, M.; Robson, R., Eds. Hydrogen as a Fuel: Learning from Nature; Taylor and Francis: London, 2001.
4. Melis, A.; Zhang, L.; Forestier, M.; Ghirardi, M. L.; Seibert, M. Plant Physiol 2000, 122, 127.
5. Albracht, S. P. J Biochim Biophys Acta 1994, 1118, 167.
6. Woodward, J.; Cordray, K. A.; Edmonston, R. J.; Blanco-Rivera, M.; Mattingly, S. M.; Evans, B. R. Energy Fuels 2000, 14, 197.
7. De Lacey, A. L.; Pardo, A.; Fernandez, V. M.; Dementin, S.; Adryanczyk-Perrier, G.; Hatchikian, E. C.; Rousset, M. J Biol Inorg Chem 2004, 9, 636.
8. De Lacey, A. L.; Detcheverry, M.; Moiroux, J.; Bourdillon, C. Biotechnol Bioeng 2000, 68, 1.
9. Borg, S. J.; Behrsing, T.; Best, S. P.; Razavet, M.; Liu, X.; Pickett, C. J. J Am Chem Soc 2004, 126, 16988.
10. Vignais, P. M.; Billoud, B.; Meyer, J. FEMS Microbiol Rev 2001, 25, 455.
11. Adams, M. W. W. Biochim Biophys Acta 1990, 1020, 115.
12. Adams, M. W. W.; Stiefel, E. I. Science 1998, 282, 1842.
13. Happe, R. P.; Roseboom, W.; Pierik, A. J.; Albracht, S. P.; Bagley, K. A. Nature 1997, 385, 126.
14. Nicolet, Y.; Cavazza, C.; Fontecilla-Camps, J. C. J Inorg Biochem 2002, 91, 1.
15. Peters, J. W.; Lanzilotta, W. N.; Lemon, B. J.; Seefeldt, L. C. Science 1998, 282, 1853.
16. Nicolet, Y.; Piras, C.; Legrand, P.; Hatchikian, E. C.; Fontecilla-Camps, J. C. Structure 1999, 7, 13.
17. Dogaru, D.; Motiu, S.; Gogonea, V. Int J Quantum Chem 2009, 109, 876.
18. Liu, Z.-P.; Hu, P. J Chem Phys 2002, 117, 8177.
19. Bruschi, M.; Fantucci, P.; De Gioia, L. Inorg Chem 2002, 41, 1421.
20. Bruschi, M.; Fantucci, P.; De Gioia, L. Inorg Chem 2003, 42, 4773.
21. Bruschi, M.; Fantucci, P.; De Gioia, L. Inorg Chem 2004, 43, 3733.
22. Zampella, G.; Bruschi, M.; Fantucci, P.; Razavet, M.; Pickett, C. J.; De Gioia, L. Chem Eur J 2005, 11, 509.
23. Cao, Z.; Hall, M. B. J Am Chem Soc 2001, 123, 3734.
24. Tye, J. W.; Darensbourg, M. Y.; Hall, M. B. Inorg Chem 2008, 47, 2380.
25. Fan, H.-J.; Hall, M. B. J Am Chem Soc 2001, 123, 3828.
26. Greco, C.; Bruschi, M.; De Gioia, L.; Ryde, U. Inorg Chem 2007, 46, 5911.
27. Trohalaki, S.; Pachter, R. Energy Fuel 2007, 21, 2278.
28. Greco, C.; Bruschi, M.; Heimdal, J.; Fantucci, P.; De Gioia, L.; Ryde, U. Inorg Chem 2007, 46, 7256.
29. Greco, C.; Bruschi, M.; Fantucci, P.; De Gioia, L. Eur J Inorg Chem 2007, 13, 1835.
30. Greco, C.; Zampella, G.; Bertini, L.; Bruschi, M.; Fantucci, P.; De Gioia, L. Inorg Chem 2007, 46, 108.

31. Motiu, S.; Dogaru, D.; Gogonea, V. Int J Quantum Chem 2007, 107, 1248.
32. Bruschi, M.; Zampella, G.; Fantucci, P.; De Gioia, L. Coord Chem Rev 2005, 15–16, 1620.
33. Liu, X.; Ibrahim, S. K.; Tard, C.; Pickett, C. J. Coord Chem Rev 2005, 15–16, 1641.
34. Armstrong, F. A. Curr Opin Chem Biol 2004, 8, 133.
35. Rauchfuss, T. B. Inorg Chem 2004, 43, 14.
36. Evans, D. J.; Pickett, C. J. Chem Soc Rev 2003, 35, 268.
37. Chen, Z.; Lemon, B. J.; Huang, S.; Swartz, D. J.; Peters, J. W.; Bagley, K. A. Biochemistry 2002, 41, 2036.
38. Horner, D. S.; Heil, B.; Happe, T.; Embley, T. M. Trends Biochem Sci 2002, 27, 148.
39. Borg, S. J.; Tye, J. W.; Hall, M. B.; Best, S. P. Inorg Chem 2007, 46, 384.
40. Zilberman, S.; Stiefel, E. I.; Cohen, M. H.; Car, R. Inorg Chem 2007, 46, 1153.
41. Tye, J. W.; Darensbourg, M. Y.; Hall, M. B. J Mol Struct (THEOCHEM) 2006, 771, 123.
42. Eilers, G.; Schwartz, L.; Stein, M.; Zampella, G.; De Gioia, L.; Ott, S.; Lomoth, R. Chem Eur J 2007, 13, 7075.
43. Lyon, E. J.; Georgakaki, I. P.; Reibenspies, J. H.; Darensbourg, M. Y. Angew Chem Int Ed 1999, 38, 3178.
44. Cloirec, A. L.; Best, S. P.; Borg, S.; Davies, S. C.; Evans, D. J.; Hughes, D. L.; Pickett, C. J. Chem Commun 1999, 2285.
45. Rauchfuss, T. B.; Contakes, S. M.; Schmidt, M. J Am Chem Soc 1999, 121, 9736.
46. Lai, C.-H.; Lee, W.-Z.; Miller, M. L.; Reibenspies, J. H.; Darensbourg, D. J.; Darensbourg, M. Y. J Am Chem Soc 1998, 120, 10103.
47. Pierik, A. J.; Hagen, W. R.; Redeker, J. S.; Wolbert, R. B. G.; Boersma, M.; Verhagen, M. F.; Grande, H. J.; Veeger, C.; Mustsaers, P. H. A.; Sand, R. H.; Dunham, W. R. Eur J Biochem 1992, 209, 63.
48. Zambrano, I. C.; Kowal, A. T.; Mortenson, L. E.; Adams, M. W. W.; Johnson, M. K. J Biol Chem 1989, 264, 20974.
49. Patil, D. S.; Moura, J. J.; He, S. H.; Teixeira, M.; Prickril, B. C.; DerVartanian, D. V.; Peck, H. D., Jr.; LeGall, J.; Huynh, B. H. J Biol Chem 1988, 263, 18732.
50. Rusnak, F. M.; Adams, M. W. W.; Mortenson, L. E.; Munck, E. J Biol Chem 1987, 262, 38.
51. Adams, M. W. W. J Biol Chem 1987, 262, 15054.
52. Adams, M. W. W.; Mortenson, L. E. J Biol Chem 1984, 259, 7045.
53. Rappe, A. K.; Casewit, C. J.; Colwell, K. S.; Goddard, W. A.; Skiff, W. M. J Am Chem Soc 1992, 113, 10024.
54. Dapprich, S.; Komaromi, I.; Byun, K. S.; Morokuma, K.; Frisch, M. J. J Mol Struct (THEOCHEM) 1999, 461, 1.
55. Frisch, M. J.; Trucks, G. W.; Schlegel, H. B.; Scuseria, G. E.; Robb, M. A.; Cheeseman, J. R.; Montgomery, J. A., Jr.; Vreven, T.; Kudin, K. N.; Burant, J. C.; Millam, J. M.; Iyengar, S. S.; Tomasi, J.; Barone, V.; Mennucci, B.; Cossi, M.; Scalmani, G.; Rega, N.; Petersson, G. A.; Nakatsuji, H.; Hada, M.; Ehara, M.; Toyota, K.; Fukuda, R.; Hasegawa, J.; Ishida, M.; Nakajima, T.; Honda, Y.; Kitao, O.; Nakai, H.; Klene, M. L., X.; Knox, J. E.; Hratchian, H. P.; Cross, J. B.; Bakken, V.; Adamo, C.; Jaramillo, J.; Gomperts, R.; Stratmann, R. E.; Yazyev, O.; Austin, A. J.; Cammi, R.; Pomelli, C.; Ochterski, J. W.; Ayala, P. Y.; Morokuma, K.; Voth, G. A.; Salvador, P.; Dannenberg, J. J.; Zakrzewski, V. G.; Dapprich, S.; Daniels, A. D.; Strain, M. C.; Farkas, O.; Malick, D. K.; Rabuck, A. D.; Raghavachari, K.; Foresman, J. B.; Ortiz, J. V.; Cui, Q.; Baboul, A. G.; Clifford, S.; Cioslowski, J.; Stefanov, B. B.; Liu, G.; Liashenko, A.; Piskorz, P.; Komaromi, I.; Martin, R. L.; Fox, D. J.; Keith, T.; Al-Laham, M. A.; Peng, C. Y.; Nanayakkara, A.; Challacombe, M.; Gill, P. M. W.; Johnson, B.; Chen, W.; Wong, M. W.; Gonzalez, C.; Pople, J. A. Gaussian 03, Revision C. 02; Gaussian, Inc.: Wallingford, CT, 2004.
56. Becke, A. D. J Chem Phys 1993, 98, 5648.
57. Lee, C.; Yang, W.; Parr, R. G. Phys Rev B 1988, 37, 785.
58. Berendsen, H. J. C.; van der Spoel, D. Comput Phys Commun 1995, 91, 43.
59. Lindahl, E.; Hess, B. J Mol Mod 2001, 7, 306.
60. Popescu, C. V.; Munck, E. J Am Chem Soc 1999, 121, 7877.
61. Rappe, A. K.; Goddard, W. A. J Phys Chem 1991, 95, 3358.
62. Peters, J. W. Curr Opin Struct Biol 1999, 9, 670.